Syntheses, Structures, and Catalytic Reactions of Palladium Adducts of Chiral Diphosphines That Contain a Rhenium Stereocenter in the Backbone

by **Klemenz Kromm**, **Frank Hampel**, and **J. A. Gladysz***

Institut für Organische Chemie, Friedrich-Alexander-Universität Erlangen-Nürnberg, Henkestrasse 42, D-91054 Erlangen

Dedicated to the memory of Professor *Luigi M. Venanzi*, a pioneer in the chemistry of group-10 diphosphine chelate complexes

Reactions of the title diphosphines [(η^5-$C_5H_4PPh_2$)Re(NO)(PPh_3)((CH_2)$_n$$PPh_2$)] ($n=0$, (*R*)-**1**; $n=1$, racemic or (*S*)-**2**) with [$PdCl_2$(PhCN)$_2$] give the palladium/rhenium chelate complexes [(η^5-$C_5H_4PPh_2$)Re(NO)(PPh_3)((μ-CH_2)$_n$$PPh_2$)$PdCl_2$] ($n=0$, (*S*)-**5**; $n=1$, racemic or (*S*)-**6**) in 75–92% yield. The crystal structure of racemic **6** shows a twisted-boat conformation of the chelate ring, giving a chiral pocket very different from that in a related rhodium chelate. However, NOE experiments suggest a similar ensemble of conformations in solution. Catalysts are generated from various combinations of *a*) $Pd(OAc)_2$ and (*R*)-**1** or (*S*)-**2** (1:2), *b*) (*S*)-**5** or (*S*)-**6** and (*R*)-**1** or (*S*)-**2** (1:2), or *c*) (i-Bu)$_2$AlH with the preceding recipes. These factors effect the *Heck* arylation of 2,3-dihydrofuran with phenyl trifluoromethylsulfonate. In contrast to analogous reactions with (*R*)-binap (=(*R*)-2,2′-bis(diphenylphosphanyl)-1,1′-binaphthalene), the major product 2-phenyl-2,3-dihydrofuran is nearly racemic ($\leq$12% ee).

Introduction. – The synthesis of chiral ferrocene-based chelating ligands and applications of their metal complexes as catalysts for enantioselective organic synthesis has seen rapidly increasing attention over the last decade [1]. Many spectacularly successful reactions have been developed, and, more recently, efforts have been extended to nonferrocene metal fragments [2–4]. Besides the direct extrapolation of ruthenocenes [1a] and our own work detailed below [3][4], examples include [Cr(η^6-arene)$(CO)_3$] [2b,c], [M(η^5-C_5R_5)$(CO)_3$] (M=Mn, Re) [2a,d,e], and [Co(η^4-C_4R_4)(η^5-C_5R_5)] [2f] derived systems. In accord with the diverse architectural possibilities inherent in such templates, all three types of stereogenic elements (centers, planes, and axes) have been employed, often in combination.

Many types of chelating diphosphines have been described that are chiral by virtue of carbon or phosphorus stereocenters [5]. We reported the first family of chelating diphosphines that are chiral by virtue of a transition-metal stereocenter, as depicted in the structures of **1** and **2** [3], which feature a chiral rhenium fragment in the backbone and are easily obtained in enantiomerically pure form. Rhodium adducts of the structures **3** and **4** were prepared and were found to be excellent catalyst precursors for the asymmetric hydrogenation of protected dehydroamino acids. Catalyst activities, lifetimes, and enantioselectivities compared well with the best systems in the literature [3].

We sought to extend the applicability of this new family of diphosphines to a wider set of chelated metal fragments and catalytic reactions. In this paper, we report the

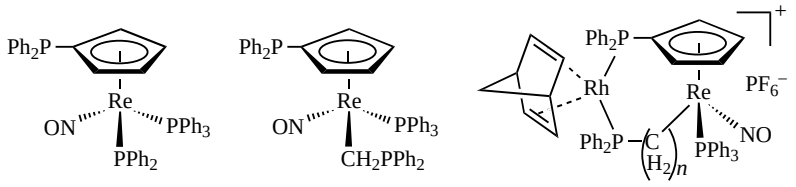

(*R*)-**1** (*S*)-**2** (*S*)-**3** (*n* = 0)
(*S*)-**4** (*n* = 1)

synthesis of two palladium chelates, the structural characterization of one in solution and in the solid state, and preliminary screening results that establish their viability as catalyst precursors for C–C bond forming reactions. The synthesis and crystal structure of a palladium chelate of a dirhenium-containing diamine, in which the Re-atoms are located in the *N*-alkyl substituents as opposed to the backbone, have been described elsewhere [4].

Results. – As shown in *Scheme 1*, (*R*)-**1** as well as racemic and (*S*)-**2** were treated each with $[PdCl_2(PhCN)_2]$ in THF[1]). Work-up gave the heterobimetallic palladium/rhenium complexes, (*S*)-$[(\eta^5\text{-}C_5H_4PPh_2)Re(NO)(PPh_3)(\mu\text{-}PPh_2)PdCl_2]$ ((*S*)-**5**) and racemic and (*S*)-$[(\eta^5\text{-}C_5H_4PPh_2)Re(NO)(PPh_3)(\mu\text{-}CH_2PPh_2)PdCl_2]$ (racemic and (*S*)-**6**), as air-stable, red or orange powders in 85–75% yield. The compounds were characterized by IR and NMR (^1H, ^{13}C, ^{31}P) spectroscopy, as summarized in the *Exper. Part* and *Table 1*. The racemate gave a correct microanalysis, but the nonracemic complexes were more difficult to purify, consistent with the lower crystallinity commonly encountered with such chiral Re compounds.

Scheme 1. *Synthesis of Palladium Chelate Complexes*[1])

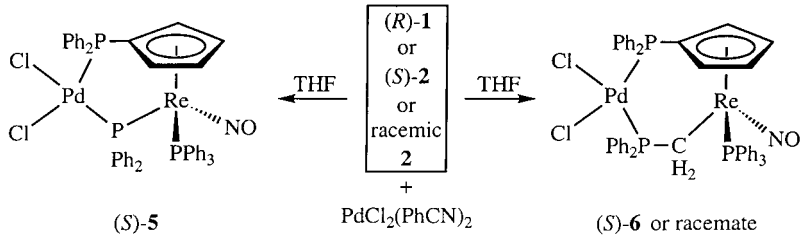

(*S*)-**5** $PdCl_2(PhCN)_2$ (*S*)-**6** or racemate

The spectroscopic properties fully supported the proposed structures. MS gave molecular ions with the correct masses and isotope distributions. NMR spectra showed distinct ^1H- and ^{13}C-signals for all cyclopentadienyl H- and C-atoms, and the former could be assigned as described below. As illustrated in *Table 1*, the ^{31}P-NMR spectra

---

[1]) The enantiomers of diphosphines **1** and **2** used to prepare nonracemic chelates have configurations opposite to those depicted in previous papers in this series. For ease of comparison, the configurations of all compounds and catalysis products have been inverted in the text, *Schemes*, and *Figures*. The true configurations are given in the *Exper. Part*. The basis for assignment of (*R*/*S*) descriptors has been summarized earlier [3a].

Table 1. *Summary of $^{31}P\{^1H\}$-NMR Data*[a])

Complex	$RePPh_3$	$Re(CH_2)_nPPh_2X$	$C_5H_4PPh_2X'$
1[b])[c])	20.2 (*d*, ^2J(P,P) = 15)	− 45.2 (*d*, ^2J(P,P) = 15)	− 16.2 (*s*)
3[c])[d])[e])	9.8 (*dd*, ^2J(P,P) = 14, ^3J(P,P) = 5)	− 49.2 (*ddd*, ^1J(P,Rh) = 127, ^2J(P,P) = 19, ^2J(P,P) = 14)	50.4 (*ddd*, ^1J(P,Rh) = 183, ^2J(P,P) = 19, ^3J(P,P) = 5)
5[f])[g])	9.1 (*s*)	− 19.1 (*d*, ^2J(P,P) = 14)	53.3 (*d*, ^2J(P,P) = 14)
2[g])[h])	26.3 (*d*, ^3J(P,P) = 8)	6.9 (*dd*, ^3J(P,P) = 3, ^3J(P,P) = 8)	− 17.7 (*d*, ^3J(P,P) = 3)
4[c])[f])[g])	20.2 (*dd*, ^3J(P,P) = 18, ^3J(P,P) = 4)	50.5 (*ddd*, ^1J(P,Rh) = 148, ^2J(P,P) = 34, ^3J(P,P) = 18)	23.9 (*ddd*, ^1J(P,Rh) = 166, ^2J(P,P) = 34, ^3J(P,P) = 4)
6[d])[g])	26.2 (*s*)	62.5 (*d*, ^2J(P,P) = 19)	21.1 (*d*, ^2J(P,P) = 19)

[a]) At r.t.; *J* in Hz. [b]) In (D_8)THF. [c]) 121 MHz. [d]) In CD_2Cl_2. [e]) − 144.0 (*sept.*, J(P,F) = 708). [f]) In $CDCl_3$. [g]) 162 MHz. [h]) In C_6D_6.

showed diagnostic chemical-shift and coupling-constant patterns, similar to those of the cationic rhodium/thenium complexes **3** and **4** [3]. With (*S*)-**5**, the signal of $C_5H_4PPh_2$ was shifted further downfield from that of the uncomplexed diphosphine ($\delta = 53.3$ *vs.* -16.2) than with racemic or (*S*)-**6** ($\delta = 21.1$ *vs.* -17.7). In contrast, the $RePPh_2$ signal of (*S*)-**5** was shifted downfield by a smaller value ($\delta = -19.1$ *vs.* -45.2) than the $ReCH_2PPh_2$ signal in racemic and (*S*)-**6** ($\delta = 62.5$ *vs.* 6.9). The cationic complex **3** gives an opposite chemical-shift trend ($\delta = -49.2$ *vs.* -45.2).

Orange needles of a solvate of racemic **6** were grown from CH_2Cl_2/hexane. The crystal structure was determined as described in *Table 2* and the *Exper. Part*. The structure is given in *Fig. 1* and confirms the above assignment. Key bond lengths, bond angles, and torsion angles are summarized in *Table 3*, and selected conformational features are analyzed below.

Palladium chelates of diphosphines are widely used in catalysis [6–8]. In some protocols, they are first isolated and purified, and, in other cases, they are simply generated *in situ*. Both approaches have advantages. For initial screening purposes, the

Table 2. *Crystallographic Data of* **6**·*3 CH_2Cl_2*

Empirical formula	$C_{51}H_{47}Cl_8NOP_3PdRe$	D (calc.) [g cm^{-3}]	1.66
M_r [g mol^{-1}]	1359.1	Absorption coefficient [mm^{-1}]	3.082
T [K]	173(2)	Crystal dimensions [mm]	0.30 × 0.25 × 0.25
Diffractometer	*Nonius KappaCCD*	Θ range [°]	≤ 25
Wavelength [Å]	0.71073	Range/indices (h,k,l)	$-13 \le h \le 13$, $-16 \le k \le 16$, $-22 \le l \le 22$
Crystal system	triclinic	Reflections collected	17185
Space group	$P\bar{1}$	Unique reflections	9289
Unit cell dimensions:			
a [Å]	11.282(2)	Reflections observed ($I > 2\sigma(I)$)	7729
b [Å]	13.738(3)	Refined parameters	594
c [Å]	18.879(4)	Refinement	least squares on F^2
α [°]	92.48(3)	R_{int}	0.0358
β [°]	93.34(3)	R indices ($I > 2\sigma(I)$)	$R_1 = 0.0723$, $wR_2 = 0.1581$
γ [°]	111.48(3)	R indices (all data)	$R_1 = 0.0871$, $wR_2 = 0.1648$
V [Å^3]	2711.7(9)	Goodness-of-fit	1.121
Z	2	Largest diff. peak and hole [e·Å^{-3}]	2.961 and − 1.848

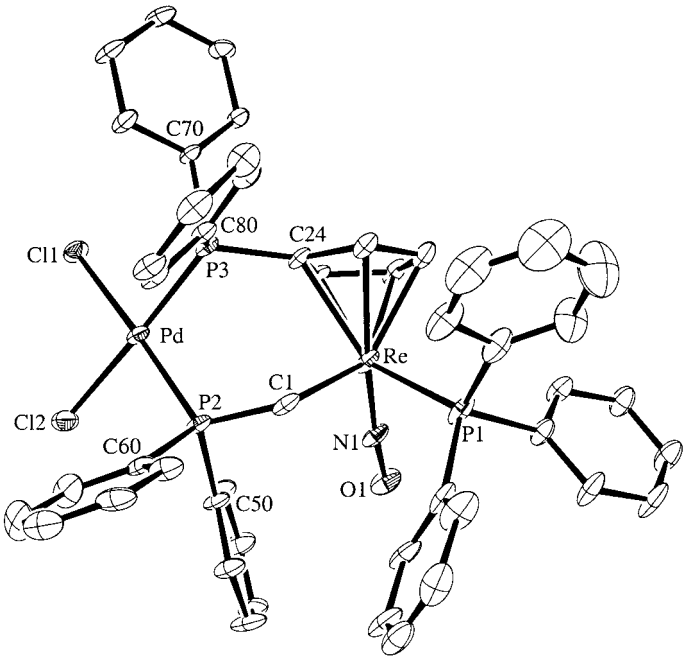

Fig. 1. *Structure of* **6** · *3* CH_2Cl_2 *with solvate molecules omitted*

test reaction shown in *Scheme 2* was selected. This *Heck* arylation is commonly conducted with phenyl trifluoromethylsulfonate (PhOTf) as the limiting reactant [7–9]. Most palladium catalysts based on chelating diphosphine ligands yield mixtures of dihydrofurans, in which the 2,3-isomer (**7**) dominates over the 3,4-isomer (**8**).The former is obtained in high ee with a catalyst generated *in situ* from $Pd(OAc)_2$/(*R*)-binap (1:2 mol ratio) ((*R*)-binap = (*R*)-2,2′-bis(diphenylphospanyl)-1,1′-binaphthalene) [7a]. The base employed also affects the enantioselectivity. Therefore, we used the same base (Et_3N) in all of our experiments.

We first verified that we could obtain the range of enantioselectivities reported for the $Pd(OAc)_2$/(*R*)-binap system (*Scheme 2*, *Entry 1*) [7a]. We then examined analogous recipes derived from $Pd(OAc)_2$ and the uncomplexed diphosphines (*R*)-**1** and (*S*)-**2** (*Entries 2* and *3*). All three of these systems exhibited substantial induction periods, which in the first case has been attributed to the required generation of a Pd(0) species, with excess diphosphine serving as reductant [10]. The diphosphines (*R*)-**1** and (*S*)-**2** gave longer induction periods and somewhat slower reactions as reflected by the time and temperature data in *Scheme 2*. Additional details are provided elsewhere [11]. However, neither diphosphine gave **7** with a significant enantiomeric excess. The nonracemic **7** prepared in *Entry 1* was added to the catalyst system in *Entry 2*. After 48 h, no racemization was observed.

Experiments with the preformed palladium chelates were investigated next. Not unsurprisingly, (*S*)-**5** was not very active alone, and (*S*)-**6** gave no reaction whatsoever. As shown in *Entries 4* and *5*, combinations of the chelates and free diphosphines (*S*)-**5**/

Table 3. *Key Distances* [Å] *and Angles* [°] *of* **6**·*3 CH_2Cl_2*

Re–N(1)	1.763(9)	P(3)–C(11)	1.802(10)
Re–P(1)	2.248(3)	Pd–P(3)	2.248(3)
Re–C(1)	2.179(10)	Pd–P(2)	2.286(3)
C(1)–P(2)	1.796(12)	Re–Cl(1)	2.344(3)
Re–Cp(centroid)	1.947	Re–Cl(2)	2.341(3)
Re–C(11)	2.253(7)	Re–Pd	4.332
N(1)–Re–P(1)	88.8(3)	P(2)–Pd–P(3)	92.95(11)
N(1)–Re–C(1)	99.5(4)	P(3)–Pd–Cl(1)	89.78(10)
C(1)–Re–P(1)	88.0(3)	Cl(1)–Pd–Cl(2)	88.24(11)
Re–C(1)–P(2)	117.1(5)	Pd–P(2)–C(50)	113.3(2)
C(24)–Re–C(1)	85.5(3)	Pd–P(2)–C(60)	108.5(2)
Re–C(24)–P(3)	127.6(5)	Pd–P(3)–C(70)	111.0(2)
Pd–P(3)–C(24)	111.9(4)	Pd–P(3)–P(80)	115.1(2)
P(2)–Pd–Cl(2)	89.04(11)		
Re–C(24)–P(3)–C(70)	–173.5(6)	Re–C(1)–P(2)–Pd	–57.6(6)
Re–C(24)–P(3)–C(80)	82.4(7)	Re–C(1)–P(2)–C(50)	68.7(6)
P(1)–Re–C(1)–P(2)	–153.6(5)	Re–C(1)–P(2)–C(60)	177.4(5)
N(1)–Re–C(1)–P(2)	–65.2(6)		

Scheme 2. *Summary of Enantioselective Arylations*

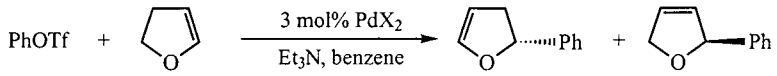

(*R*)-**7** (*S*)-**8**

Entry	Catalyst System, Conditions	Conv. [%]	Ratio (**7**:**8**)	Yield (**7**+**8**) [%]	ee (*R*)-**7** [%]
1	$Pd(OAc)_2$/(*R*)-binap (1:2), 40°, 8 d	95	88:12	72	74
2	$Pd(OAc)_2$/(*R*)-**1** (1:2), 40°, 14 d	90	78:22	75	5
3	$Pd(OAc)_2$/(*S*)-**2** (1:2), 60°, 14 d	80	92:8	69	5
4	(*S*)-**5**/(*R*)-**1** (1:2), 40°, 14 d	85	88:12	72	10
5	(*S*)-**6**/(*S*)-**2** (1:2), 60°, 8 d	60	90:10	–	5
6	(*S*)-**5**/(*R*)-**1**/$(i\text{-}Bu)_2AlH$ (1:1.5:2), 60°, 9 d	35	86:14	–	n.d.
7	(*S*)-**6**/(*S*)-**2**/$(i\text{-}Bu)_2AlH$ (1:1.5:2), 40°, 4 d	95	90:10	84	12

(*R*)-**1** or (*S*)-**6**/(*S*)-**2** (1:1 molar ratio) yielded after induction periods deep red solutions of active catalysts that again afforded low enantioselectivity. The reductant $(i\text{-}Bu)_2AlH$ is sometimes employed to generate Pd(0) species [12]. Accordingly, *Entries 6* and *7* are similar to *4* and *5*, but with 2.0 equivalents of $(i\text{-}Bu)_2AlH$. *Entry 7* gave the highest rate and enantioselectivity of all, but the latter (12% ee) was far below useful levels. Similar data were obtained with cyclohexenyl tirfluoromethylsulfonate, as detailed elsewhere [11].

The preceding data prompted us to test the conformations of **6** and of the related rhodium/rhenium complex **4** in solution by NMR with the one dimensional DPFGSE-NOE technique [13][14]. In the first series of experiments, all nonphenyl H-atom signals were separately irradiated. Each cyclopentadienyl H-atom signal irradiated gave a 1.5–2.2% enhancement of the neighboring cyclopentadienyl H-atom

signals, establishing connectivity[2]). Both **6** and **4** exhibited a high-field cyclopentadienyl H-atom signal ($\delta = 3.19$ and 4.34; designated as H_α) with only a single neighbor. Irradiation of these signals also gave enhancements of the high-field ReCHH′ H-atom signal (1.2%) but not the low-field signal (<0.1%). The reverse irradiations gave enhancements of 2.3% and 2.5%. All other NOE relationships were also very similar. Representative spectra are illustrated in *Fig. 2*. These data are analyzed (*Discussion*) in relation to the partial structures in *Fig. 3*.

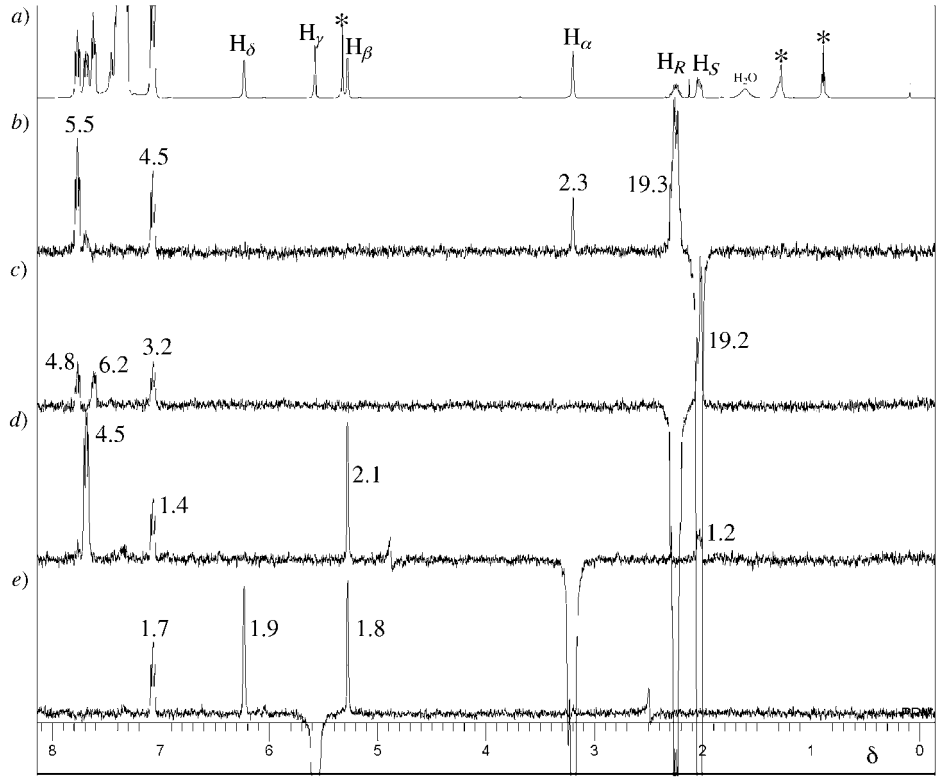

Fig. 2. *^{1}H-NMR Spectra of* **6** (CD_2Cl_2; see *Fig. 3* for definitions of the indices $\alpha - \gamma$, *R* and *S*). *a*) Standard 500-MHz spectrum (solvent impurities are designated by *); *b*) DPFGSE-NOE spectrum from the irradiation of signal H_S, with enhancements relative to the irradiated signal (−100%); *c*) as in *b*) but irradiation of signal H_R; *d*) as in *b* but irradiation of signal H_α; *e*) as in *b* but irradiation of signal H_γ.

Discussion. – The preceding data establish that the rhenium-containing diphosphines **1** and **2** readily form $PdCl_2$ chelates. Together with the previously reported rhodium chelates **3** and **4**, it can be assumed that such diphosphines will chelate a variety of metal fragments. The rotational degree of freedom intrinsic to the

[2]) Moderate enhancements of some aromatic H-atom resonances were also observed. With **4**, irradiation of the trinorbornadiene =CH H-atoms gave either enhancements of or excitation transfer to all other trinorbornadiene signals, indicating an exchange process that is further described in the *Exper. Part.*

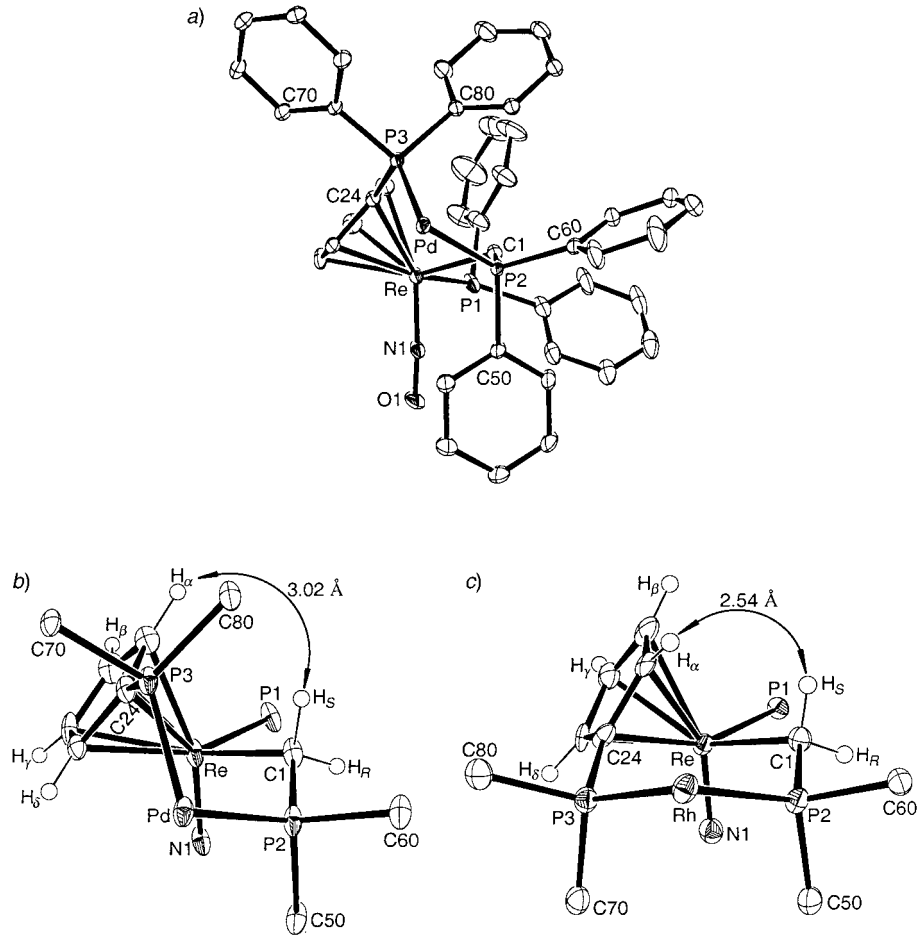

Fig. 3. *Selected conformational features of chelate complexes. a*) **6** · 3 CH_2Cl_2 with the palladium chloride ligands, one PPh_3 phenyl ring, and solvate omitted; *b*) as in *a* but with only the cyclopentadienyl C-atoms and H-atoms, (calc. positions), and immediately bonded atoms of the chelate ring; *c*) as in *b* but for rhodium complex **4**.

cyclopentadienyl-based PPh_2 group enables a wide range of PP distances and bite angles. As analyzed earlier, the $Re(CH_2)_nPPh_2$ moieties are much more basic and nucleophilic than model organic phosphines that lack the rhenium substituent [3]. Enhanced phosphine basicity, as well as steric bulk, increases the rates of many metal-catalyzed reactions [15].

As noted above, **3** and **4** were highly effective catalyst precursors for the enantioselective hydrogenation of protected dehydroamino acids. However, the palladium chelates **5** and **6**, or related species generated *in situ* with $Pd(OAc)_2$, are active but are poorly enantioselective catalyst precursors with respect to the *Heck* arylation in *Scheme 2*. No correlation would necessarily be expected, as these transformations involve much different types of configuration-determining steps, as well as catalyst electronic configuration (Rh(I)/(III) or d^8/d^6 *vs.* Pd(0)/Pd(II) or d^{10}/d^8).

In any event, this inauspicious beginning should not diminish enthusiasm for palladium catalysts derived from diphosphines **1** or **2**. The enantioselectivities of *Heck* arylations are known to be highly dependent upon a number of factors. For example, when aryl trifluoromethylsulfonates are replaced by aryl iodides, racemic or essentially racemic products are obtained [7a].

The crystal structure of **6** (*Fig. 1*) shows the normal types of bond lengths and angles about the formally octahedral Re-atom (*Table 3*) [3][4]. The P(2)–C(1) linkage bends into the interstice on the Re-atom between the least bulky nitrosyl and cyclopentadienyl ligands, as indicated by the N(1)–Re–C(1)–P(2) and P(1)–Re–C(1)–P(2) torsion angles (–65.2° and –153.6°). *Fig. 3* shows two views of the 'chiral pocket' generated by removing the Cl^- ligands from the Pd-atom (*a*, *b*). View *a* highlights the face/edge dispositions of the four phenyl groups, which have been carefully analyzed by *Brunner et al.* [5a] and which transmit chirality to the reaction site. View *b* highlights the conformation of the six-membered chelate ring and cyclopentadienyl ligand. For comparison, the analogous segment of rhodium/rhenium complex **4** is shown in view *c*.

In contrast to the chair-like conformation of the rhodium chelate in *c*, the palladium chelate in *b* adopts a folded, twist-boat-like conformation. The torsion angles about the C(1)–P(1) bonds are quite similar in both structures. Hence, the major difference stems from the rotational degree of freedom involving the substituted cyclopentadienyl ligand. In this regard, note that the C(24)–Re–C1 angle in *b* is much smaller than in *c* (85.5(3)° *vs.* 99.4(3)°). These differences lead to different categories of chiral pockets. That in **6** (see *a*) exhibits a P^3M configuration, whereas **4** shows a P^2M^2 configuration. P and M are helical chirality descriptors relating the four phenyl groups, derived by *Brunner*'s protocol [5a][3]).

The Pd–P bond lengths in *b* are close to the Rh–P bond lengths in *c* (2.248(3) – 2.286(3) *vs.* 2.295(2) – 2.360(2) Å), and the remaining bond distances are nearly identical. Therefore, the differing conformations must either represent responses to the other metal ligands (Cl^- on Pd-atom *vs.* diene on Rh-atom), or a crystal-packing effect. The close similarity of the NOE data for **6** and **4** suggests a similar ensemble of conformations in solution, supporting a packing effect. Although the palladium/rhenium chelate **5** was not structurally investigated, the diminished degrees of freedom resulting from the smaller ring size renders a close correspondence to the rhodium/rhenium analog **3** even more likely.

View *c* of **4** shows the only possible assignment of H_α that would give an enhancement of a ReCHH′ H-atom, which occupies an axial position and, when rhenium has the absolute configuration depicted in *c*, corresponds to H_S. The conformation in view *b* of **4** features a greater distance between H_α and the corresponding ReCHH′ H-atom (3.02 *vs.* 2.54 Å) and would give a much lower NOE enhancement due to the $1/r^6$ dependence. However, since there is no way to calibrate the exact value expected for each conformation, we can only conclude that the relative conformer populations are similar. The upfield chemical shifts of the H_α signals are logically attributed to the shielding effect of a PPh_3 phenyl ring.

---

[3]) A table of structural data relating to the chiral pocket defined by the PPh_2 group of **6** and **4** can be obtained from the author.

In summary, this work has extended the synthetic, structural, and catalytic chemistry of architecturally novel metal complexes derived from chiral-chelating diphosphines that contain a transition-metal stereocenter in the backbone. Although the enantioselectivities in the reaction initially explored with the new palladium/rhenium precatalyst **6** are modest, NOE experiments indicate an ensemble of conformations similar to those in the highly effective rhodium/rhenium precatalyst **4**. Chelate ligands that incorporate other types of chiral, non-ferrocene metal fragments are seeing rapid development in other groups [2]. Additional examples and applications of metal-containing donor ligands in catalysis will be reported in the near future [16].

Experimental Part

General. General procedures, chemical purifications, and instrumentation were identical with those in two recent full papers [3][4]. Chemicals new to this work were obtained and treated as follows: di(benzonitrilo)dichloropalladium($[PdCl_2(PhCN)_2]$), prepared from $PdCl_2$ (*Johnson Matthey*, 99.9%) [17]; phenyl trifluoromethylsulfonate, (PhOTf), prepared from phenol, pyridine, and trifluoromethylsulfonic acid anhydride (*Fluka*) [18]; $(i\text{-}Bu)_2AlH$ (~1.2M in toluene, *Fluka*), Et_3N (*Fluka*, 99.99%), and (+)-tris{3-[(heptafluoro)hydroxymethylene]camphorato}europium(III) ((+)-[Eu(hfc)$_3$]; *Aldrich*) were used as received.

(R)-[(η^5-$C_5H_4PPh_2$)Re(NO)(PPh_3)(μ-PPh_2)$PdCl_2$] ((*R*)-**5**[1]). A *Schlenk* flask was charged with (*S*)-[(η^5-$C_5H_4PPh_2$)Re(NO)(PPh_3)(PPh_2)] ((*S*)-**1**; 1.150 g, 1.260 mmol) [3a][1]) and THF (30 ml). A soln. of $[PdCl_2(PhCN)_2]$ (0.4833 g, 1.260 mmol) in THF (20 ml) was added with stirring. After 30 min, pentane (30 ml) was added to the purple-red heterogeneous mixture. After 60 min, the solid was collected on a sintered glass filter, washed with THF (2 × 3 ml) and pentane (2 × 10 ml), and dried *in vacuo* to give (*R*)-**5** (1.025 g, 0.9401 mmol, 75%)[1]) as a carmine powder that was >95% pure by ^{31}P-NMR. M.p. 230–235° (dec). IR (powder film, cm^{-1}): 1687*s* (NO). ^{1}H-NMR (400 MHz, $CDCl_3$): 8.18–8.13, 7.97–7.92, 7.79–7.68, 7.64–7.25, 7.15–6.96, 6.95–6.84, 6.64–6.59 (7*m*, 7 C_6H_5); 5.71, 5.63, 5.57, 4.72 (4 br. *s*, C_5H_4). ^{13}C{^{1}H}-NMR (100.5 MHz, $CDCl_3$): 142.1 (*d*, *J*(C,P) = 30, C_i (PPh_2)); 137.8 (*d*, *J*(C,P) = 30, C_i (PPh_2)); 136.1 (*d*, *J*(C,P) = 14, C_o (PPh_2)); 134.2 (*d*, *J*(C,P) = 11, C'_o (PPh_2)); 133.7 (*s*, C_p (PPh_2)); 133.7 (*d*, *J*(C,P) = 13, C''_o (PPh_2)); 133.4 (*d*, *J*(C,P) = 10.2, C'''_o (PPh_2)); 132.5 (*s*, C'_p (PPh_2)); 130.8 (*s*, C_p (PPh_3)); 130.5 (*s*, C''_p (PPh_2)); 129.0 (*s*, C'''_p (PPh_2)); 128.8 (*d*, *J*(C,P) = 12, C_m (PPh_2)); 128.5 (*d*, *J*(C,P) = 10, C_m (PPh_3)); 127.9 (*d*, *J*(C,P) = 11, C'_m (PPh_2)); 127.3 (*d*, *J*(C,P) = 10, C''_m (PPh_2)); 127.1 (*d*, *J*(C,P) = 10, C'''_m (PPh_2)); 112.9 (br. *s*, C_5H_4); 100.6 (br. *s*, C_5H_4); 98.3 (*s*, C_5H_4); 94.9 (*s*, C_5H_4); 84.2 (*s*, C_5H_4). ^{31}P{^{1}H}-NMR: see *Table 1*. FAB-MS[4]): 1090 (5, M^+), 1055 (9, $[M-Cl]^+$), 1018 (10, $[M-2Cl]^+$), 914 (9, $[M-PdCl_2]^+$), 834 (100, $[M-PdCl_2-C_6H_5]^+$), no other significant peaks above >700. Anal. calc. for $C_{47}H_{39}Cl_2NOP_3PdRe$ (1090.3): C 51.77, H 3.60, N 1.28; found: C 50.24, H 3.84, N 1.18.

[(η^5-$C_5H_4PPh_2$)Re(NO)(PPh_3)(μ-CH_2PPh_2)$PdCl_2$] (**6**). *Procedure A*. A *Schlenk* tube was charged with [Re(η^5-$C_5H_4PPh_2$)(CH_2PPh_2)(NO)(PPh_3)] (**2**; 0.0818 g, 0.0882 mmol) [3a] and THF (4 ml). A soln. of $[PdCl_2(PhCN)_2]$ (0.0338 g, 0.0882 mmol) in benzene (4 ml) was added with stirring. After 30 min, pentane (10 ml) was added to the beige heterogeneous mixture. The solid was collected on a sintered glass filter, washed with pentane (2 × 5 ml), and dried *in vacuo* (0.0789 g, 0.0714 mmol, 81%). The crude product was filtered (SiO_2, 10 × 1 cm, MeOH/CH_2Cl_2), and the filtrate was concentrated *in vacuo* to 5 ml. The precipitate was collected on a sintered glass filter, washed with pentane (5 ml), and dried *in vacuo* to give **6** as a rusty-brown powder (0.0731 g, 0.0662 mmol, 75%) that was >99% pure by ^{31}P-NMR. M.p. 215–220° (dec.). IR (powder film, cm^{-1}): 1661*s*, (NO). ^{1}H-NMR (400 MHz, $CDCl_3$)[5]): 7.94–7.31 (*m*, 7 C_6H_5): 6.22 (br. *s*, H_δ (C_5H_4)); 5.57 (br. *s*, H_γ (C_5H_4)); 5.27 (br. *s*, H_β (C_5H_4)); 3.19 (br. *s*, H_α (C_5H_4)); 2.26–2.22 (*m*, CH_RH_S): 2.05–2.00 (*m*, CH_RH_S). ^{13}C{^{1}H}-NMR (100.5 MHz, CD_2Cl_2): 138.8 (*d*, *J*(C,P) = 39, C_i (PPh_2)); 136.7 (*d*, *J*(C,P) = 12, C_o (PPh_2)); 135.5 (*d*, *J*(C,P) = 37, C'_i (PPh_2)); 135.3 (*d*, *J*(C,P) = 10, C'_o (PPh_2)); 134.1 (*d*, *J*(C,P) = 54, C_i (PPh_3)); 133.8

---

[4]) *m*/*z* Values correspond to the most intense peak of the isotope envelope; relative intensities are for the specified mass range.

[5]) The H-atoms designated α, β, γ, δ, H_S, and H_R were assigned from the NOE experiments, and the positions are defined in *Fig. 3*.

(d, J(C,P) = 8, C_o'' (PPh_2)); 133.6 (d, J(C,P) = 10, C_o (PPh_3)); 133.2 (d, J(C,P) = 10, C_o''' (PPh_2)); 132.8 (s, C_p (PPh_2)); 131.0 (s, C_p (PPh_3)); 130.7 (s, C_p' (PPh_2)); 130.5 (s, C_p'' (PPh_2)); 130.3 (s, C_p''' (PPh_2)); 129.2 (d, J(C,P) = 11, C_m (PPh_2)); 129.1 (d, J(C,P) = 11, C_m (PPh_3)); 128.1 (d, J(C,P) = 11, C_m' (PPh_2)); 128.1 (d, J(C,P) = 10, C_m'' (PPh_2)); 127.9 (d, J(C,P) = 10, C_m''' (PPh_2)); 92.3 (s, C_5H_4); 91.7 (br. s, C_5H_4); 89.0 (s, C_5H_4); 87.6 (s, C_5H_4); −9.6 (br. s, CH_2); $^{31}P\{^1H\}$-NMR: see *Table 1*. FAB-MS[4]): 1103 (2, M^+), 1068 (82, $[M-Cl]^+$), 834 (42, $[M-2Cl-CH_2PPh_2]^+$), 771 (100, $[M-2Cl-PPh_3]^+$), no other significant peaks above >700. Anal. calc. for $C_{48}H_{41}Cl_2NOP_3PdRe$ (1104.3): C 52.21, H 3.74, N 1.27; found: C 51.82, H 3.60, N 1.31.

Procedure B. A *Schlenk* tube was charged with (*R*)-**2** (0.546 g, 0.589 mmol) [3a][1]) and THF (35 ml). A soln. of $[PdCl_2(PhCN)_2]$ (0.2258 g, 0.5886 mmol) in THF (10 ml) was added with stirring. After 30 min, pentane (50 ml) was added to the beige heterogeneous mixture. The solid was collected on a sintered glass filter, washed with pentane (2 × 5 ml), and dried *in vacuo* (0.5980 g, 0.5415 mmol, 92%). The crude product was dissolved in CH_2Cl_2 (10 ml) and layered with hexane (40 ml). After 24 h, the orange needles were collected by filtration, washed with pentane (2 × 4 ml) and dried (10^{-3} bar, 2 h) to give (*R*)-**6** (0.5525 g, 0.5003 mmol, 85%)[1]) that was >99% pure by ^{31}P-NMR. M.p. 212–214° (dec.) $[\alpha]_{26}^{589} = -127 \pm 3$ (c = 1.20, THF). The NMR spectra (^1H, ^{13}C, ^{31}P) were similar to those of the racemate. Anal. calc. for $C_{48}H_{41}Cl_2NOP_3PdRe$ (1104.3): C 52.21, H 3.74, N 1.27; found: C 51.61, H 4.00, N 1.20.

Representative Catalytic Reactions. Reaction A. A 5-ml vial was charged under Ar with $Pd(OAc)_2$ (0.007 g, 0.031 mmol), (*S*)-**1** or (*R*)-**2** (0.060 mmol)[1]), benzene (2 ml), and undecane standard (typically 0.078 g, 0.500 mmol), capped with a septum, and heated with stirring in a sand bath (*Scheme 2*). A brown precipitate formed. After 20 min, PhOTf (0.226 g, 1.00 mmol), Et_3N (0.202 g, 2.00 mmol), and 2,3-dihydrofuran (0.351 g, 5.00 mmol) were added. The vial was sealed under Ar, and the heterogeneous mixture was stirred until reaction was complete (GLC, *Optima-5*, *Macherey-Nagel*, 25 μm, 25 m × 0.32 mm; 100–180°, 20°/min). t_r: 3.9 min (PhOTf), 5.7 min (undecane), 7.8 min (2,3-dihydro-2-phenylfuran (**7**)), 8.3 min (2,5-dihydro-2-phenylfuran (**8**)). The mixture was poured into pentane (10 ml) and filtered (SiO_2, 1 × 5 cm, pentane). The combined eluates were concentrated, and the yellow oil was purified by FC (SiO_2, 2 × 15 cm, pentane/ether 1:1) to afford a mixture of **7** and **8** as a colorless oil. The enantiomeric purity of **7** was elucidated with the shift reagent (+)-[Eu(hfc)$_3$] (^1H-NMR, $CDCl_3$: olefinic and aliphatic signals of (*S*)-**7** downfield from (*R*)-**7**) [7a].

Reaction B. A 5-ml vial was charged under Ar with (*R*)-**5** or (*R*)-**6** (0.030 mmol)[1]), (*S*)-**1** or (*R*)-**2** (0.060 mmol)[1]), and benzene (2 ml), capped with a septum, and heated with stirring in a sand bath (*Scheme 2*). After 20 min, PhOTf (0.226 g, 1.00 mmol), Et_3N (0.202 g, 2.00 mmol), and 2,3-dihydrofuran (0.351 g, 5.00 mmol) were added. The reaction was monitored and worked up as described for *Reaction A*.

Reaction C. A 5-ml vial was charged under Ar with (*R*)-**6** (0.0430 g, 0.0389 mmol)[1]), (*R*)-**2** (0.0541 g, 0.0584 mmol)[1]) and benzene (3 ml), capped with a septum, and heated with stirring in a sand bath. After 5 min, (i-Bu)$_2$AlH (0.065 ml, 0.0778 mmol; 1.2M in toluene) was added dropwise with stirring. Gas bubbles formed and the mixture immediately turned deep red. Then, PhOTf (0.294 g, 1.30 mmol), Et_3N (0.263 g, 2.6 mmol), and 2,3-dihydrofuran (0.456 g, 6.50 mmol) were added, and the homogeneous mixture was stirred at 40°. The reaction was monitored and worked up as described for *Reaction A*.

Crystallography. A CH_2Cl_2 soln. of **6** was layered with hexanes. After 1 d at r.t., orange needles of **6**·3 CH_2Cl_2 had formed. Data were collected as outlined in *Table 2*. Cell parameters were obtained from 10 frames with a 10° scan and refined with 53094 reflections. *Lorentz*, polarization, and absorption corrections [19] were applied. The space group was determined from systematic absences and subsequent least-squares refinement. The structure was solved by direct methods. The parameters were refined with all data by full-matrix least-squares on F^2 by means of SHELXL-97 [20]. Non-H-atoms were refined with anisotropic thermal parameters. The H-atoms were fixed in idealized positions by means of a riding model. Scattering factors were taken from the literature [21]. The asymmetric unit contained 3 molecules of CH_2Cl_2. Two were disordered and refined to occupancy ratios of 51:49 (C91/C91′, Cl3/Cl3′, Cl4/Cl4′) and 60:40 (Cl5/Cl5′, Cl6/Cl6′).

Crystallographic data (excluding structure factors) have been deposited with the *Cambridge Crystallographic Data Centre*, No. CCDC 176280. Copies of this information can be obtained, free of charge, on application to CCDC, 12 Union Road, Cambridge CB2 1EZ UK (fax: +44(1223)336033; e-mail: deposit@ccdc.ca.ac.uk).

NOE Experiments. A 5-mm NMR tube was placed in a *Schlenk* tube, evacuated, heated, purged with N_2, and charged with a soln. of **4**·CH_2Cl_2 or **6** (0.0158 mmol) in dry $CDCl_3$ or CD_2Cl_2 (0.7 ml; 0.022M). The soln. was purged with a gentle N_2 stream (10 min). The tube was sealed with a *Teflon* septum and transferred to a *JEOL Alpha-500* spectrometer for DPFGSE-NOE measurements [13][14]. Chemical shifts were referenced to residual solvent ^1H-signals (δ = 7.27, $CDCl_3$; 5.32, CH_2Cl_2). The data allowed additional assignments for the previously reported **4**·CH_2Cl_2 [3] ($CDCl_3$, 24°)[5]): 5.55 (br. s, H_δ (C_5H_4)); 5.51 (br. s, H_γ (C_5H_4)); 4.92 (br. s,

=CH (trinorbornadiene)); 4.89 (br. *s*, H_β (C_5H_4)); 4.63, 4.54 (2 br. *s*, 2 =CH (trinorbornadiene)); 4.10 (br. *s*, =CH (trinorbornadiene)); 4.02, 3.85 (2 br. *s*, 2 bridgehead CH); 1.52 (br. *s*, C*HH'*); 2.38–2.28 (*m*, CH_RH_S); 2.23–2.18 (*m*, CH_RH_S). A ^{1}H-NOESY/EXSY experiment showed cross peaks for three pairs of signals (4.92/4.10, 4.63/4.54, 4.02/3.85), consistent with a well-precedented exchange involving a *formal* 180° rotation about the rhodium-trinorbonadiene bond axis[6]).

We thank the *Deutsche Forschungsgemeinschaft* (*DFG*, GL 300/4-1), Dr. *Walter Bauer* for assistance with the NOE measurement, and *Johnson Matthey PMC* (palladium loan) for support.

REFERENCES

[1] a) A. Togni, in 'Metallocenes', Eds. A. Togni, R. L. Halterman, Wiley-VCH, Weinheim, 1998, Vol. 2, Chapt. 10; b) C. J. Richards, A. J. Locke, *Tetrahedron: Asymmetry* **1998**, *9*, 2377; c) A. Togni, N. Bieler, U. Burckhardt, C. Köllner, G. Pioda, R. Schneider, A. Schnyder, *Pure Appl. Chem*. **1999**, *71*, 1531; d) D. A. Dobbs, K. P. M. Vanhessche, E. Brazi, V. Rautenstrauch, J.-Y. Lenoir, J.-P. Genêt, J. Wiles, S. H. Bergens, *Angew. Chem.* **2000**, *112*, 2080; *Angew. Chem., Int. Ed*. **2000**, *39*, 1992.

[2] a) S. Kudis, G. Helmchen, *Angew. Chem*. **1998**, *110*, 3210; *Angew. Chem., Int. Ed*. **1998**, *37*, 3047; b) C. Bolm, K. Muñiz, *Chem. Soc. Rev.* **1999**, *28*, 51; c) C. Pasquier, L. Pélinski, J. Brocard, A. Mortreux, F. Agbossou-Niedercorn, *Tetrahedron Lett*. **2001**, *42*, 2809; d) S. U. Son, K. H. Park, S. J. Lee, Y. K. Chung, D. A. Sweigart, *Chem. Commun*. **2001**, 1290; e) C. Bolm, M. Kesselgruber, N. Hermanns, J. P. Hildebrand, G. Raabe, *Angew. Chem*. **2001**, *113*, 1536; *Angew. Chem., Int. Ed*. **2001**, *40*, 1488; f) G. Jones, C. J. Richards, *Organometallics* **2001**, *20*, 1251.

[3] a) K. Kromm, B. D. Zwick, O. Meyer, F. Hampel, J. A. Gladysz, *Chem. – Eur. J.* **2001**, *7*, 2015; b) B. D. Zwick, A. M. Arif, A. T. Patton, J. A. Gladysz, *Angew. Chem*. **1987**, *99*, 921; *Angew. Chem., Int. Ed.* **1987**, *26*, 910.

[4] L. J. Alvey, O. Delacroix, C. Wallner, O. Meyer, F. Hampel, S. Szafert, T. Lis, J. A. Gladysz, *Organometallics* **2001**, *20*, 3087.

[5] a) H. Brunner, A. Winter, J. Breu, *J. Organomet. Chem.* **1998**, *553*, 285; b) T. Ohkuma, M. Kitamura, R. Noyori, in 'Catalytic Asymmetric Synthesis' 2nd edn., Ed. I. Ojima, Wiley-VCH, Weinheim, 2000. Chapt. 1.

[6] 'Transition Metals for Organic Synthesis', Eds. M. Beller, C. Bolm, Wiley-VCH, Weinheim, 1998, Vol. 1–2; A. Tenaglia, A. Heumann, *Angew. Chem.* **1999**, *111*, 2316; *Angew. Chem., Int. Ed*. **1999**, *38*, 2180; S. A. Raynor, J. M. Thomas, R. Raja, B. F. G. Johnson, R. G. Bell, M. D. Mantle, *Chem. Commun*. **2000**, 1925.

[7] a) F. Ozawa, A. Kubo, Y. Matsumoto, T. Hayashi, E. Nishioka, K. Yanagi, K. Moriguchi, *Organometallics* **1993**, *12*, 4188, and earlier refs. cited therein; b) Y. Hashimoto, Y. Horie, M. Hayashi, K. Saigo, *Tetrahedron: Asymmetry* **2000**, *11*, 2205.

[8] O. Loiseleur, P. Meier, A. Pfaltz, *Angew. Chem.* **1996**, *108*, 218; *Angew. Chem., Int. Ed.* **1996**, *35*, 200; O. Loiseleur, M. Hayashi, N. Schmees, A. Pfaltz, *Synthesis* **1997**, 1338.

[9] S. R. Gilbertson, Z. Fu, D. Xie, *Tetrahedron Lett*. **2001**, *42*, 365, and earlier refs. cited therein.

[10] F. Ozawa, A. Kubo, T. Hayashi, *Chem. Lett*. **1992**, 2177.

[11] K. Kromm, PhD Thesis, Universität Erlangen-Nürnberg, in preparation.

[12] E. Negishi, R. A. John, *J. Org. Chem*. **1983**, *48*, 4098.

[13] K. Stott, J. Keeler, Q. N. Van, A. J. Shaka, *J. Mag. Res.* **1997**, *125*, 302.

[14] W. Bauer, A. Soi, A. Hirsch, *Magn. Reson. Chem.* **2000**, *38*, 500; C. Gaul, P. I. Arvidsson, W. Bauer, R. E. Gawley, D. Seebach, *Chem. – Eur. J.* **2001**, *7*, 4117.

[15] Q. Shelby, N. Kataoka, G. Mann, J. Hartwig, *J. Am. Chem. Soc*. **2000**, *122*, 10718; K. E. Torraca, S.-I. Kuwabe, S. L. Buchwald, *J. Am. Chem. Soc*. **2000**, *122*, 12907; C. Dai, G. C. Fu, *J. Am. Chem. Soc*. **2001**, *123*, 2719; G. Y. Li, *Angew. Chem.* **2001**, *113*, 1561; *Angew. Chem., Int. Ed.* **2001**, *40*, 1513.

[16] S. Eichenseher, K. Kromm, O. Delacroix, J. A. Gladysz, *Chem. Commun.* **2002**, 1046; K. Kromm, P. L. Osburn, J. A. Gladysz, submitted for publication.

[17] 'Synthetic Methods of Organometallic and Inorganic Chemistry', Eds. W. A. Herrmann, A. Salzer, Thieme, Stuttgart, 1996, Vol. 1, p. 159–160.

[18] M. E. Mowery, P. DeShong, *J. Org. Chem*. **1999**, *64*, 3266; L. R. Subramanian, M. Hanack, L. W. K. Chang, M. A. Imhoff, P. v. R. Schleyer, F. Effenberger, W. Kurtz, P. J. Stang, T. E. Dueber, *J. Org. Chem*. **1976**, *26*, 4099; E. Anders, M. Stankowiak, *Synthesis* **1984**, 1039.

---

6) The actual mechanism is known to be more complex [22].

[19] 'Collect'. Data collection software, Nonius B. V., 1998; Z. Otwinowski, W. Minor, *Methods Enzymol*. **1997**, *276*, 307.
[20] G. M. Sheldrick, SHELX-97, Program for refinement of crystal structures, University of Göttingen, 1997.
[21] D. T. Cromer, J. T. Waber, in 'International Tables for X-Ray Crystallography', Eds. J. A. Ibers, W. C. Hamilton, Kynoch; Birmingham, 1974.
[22] H. Berger, R. Nesper, P. S. Pregosin, H. Rüegger, M. Wörle, *Helv. Chim. Acta* **1993**, *76*, 1520; M. Valentini, K. Selvakumar, M. Wörle, P. S. Pregosin, *J. Organomet. Chem*. **1999**, *587*, 244; B. Crociani, S. Antonaroli, M. L. Di Vona, S. Licoccia, *J. Organomet. Chem*. **2001**, *631*, 117.

Received December 21, 2001